



## Corrosion protection of copper by L-arginine

S. Geethalakshmi<sup>1</sup>, S. Rajendran<sup>2</sup>, V. Palanivel<sup>2\*</sup>, A. Faritha<sup>2</sup> and T. Kasilingam<sup>2</sup>

<sup>1</sup>Govt. High School, Manakkudi, Ariyalur, Tamil Nadu, India

<sup>2</sup>PG & Research Department of Chemistry, Periyar E. V. R. College (Autonomous), Tiruchirappalli, TN, India

### ABSTRACT

*In the present study L-Arginine was used against the corrosion of copper in 0.5M HNO<sub>3</sub> solution are made using potentiodynamic polarization, electrochemical impedance spectroscopy and weight loss techniques. The results of potentiodynamic polarization technique showed that the protector is mixed type. Data obtained from impedance spectra were analyzed with model inhibition process through appropriate equivalent circuit models. The quantum chemical calculations explain the good protector of L-Arginine on the copper surface and enhance the inhibition efficiency. Simple approach was developed for generating hydrophobic surface modification of copper. Induced by the lotus effect in which water droplets falling on the leaves bead up and roll off, copper immersed in 0.5M HNO<sub>3</sub> in the presence of L-Arginine was attempted to create hydrophobic surfaces. However, the water contact angle on presence of protector was found to be 142° ± 4°, whereas in the case of copper, it was 85° ± 2°. A detailed description of the modified hydrophobic surface in 0.5M HNO<sub>3</sub> on copper is presented in this article.*

**Keywords:** Quantum chemical calculations, Water contact angle, Electrochemical studies and Surface studies

### INTRODUCTION

Copper is one of the most essential metals owing to its huge industrial applications, such as electronics, etc. It is commonly a relatively noble metal; however, it is susceptible to corrosion by acids and strong alkaline solutions, especially in the presence of oxygen or oxidants. Copper is one of the most significant nonferrous materials [1, 2]. In the pH range between 2 and 5, the dissolution of Cu is very rapid, and the formation of a stable surface oxide layer, which can passivate metal surfaces, is hindered. An oxide surface layer can only be formed in weak acid or alkaline solutions. The behaviour of Cu in acidic media is extensively investigated and several schemes have been presented for the dissolution process [3-7].

Furthermore, copper and copper-based machinery may be deployed in service environments where they may get in contact with acid solutions or fumes [8-10]. To minimize the metal dissolution under such conditions, several approaches have been exploited [11-13]. Among the corrosion protection methods available, the use of organic inhibitors has proved to be effective and efficient [14-18]. The use of polymers (natural and synthetic) as organic inhibitors for metal corrosion in aggressive environments has received much attention recently [19-32]. Generally, polymers form elastic films when in solution. As inhibitors, they films get adsorbed on the metal surface and form protective barrier to corrosive environments, thereby reducing the corrosion susceptibility of the metal surface [19, 29]. Consequently, the service life of the metal is prolonged. Reports show that the inhibitive properties of polymers are owing to the presence of hetero-atoms such as nitrogen, N<sup>-</sup>; sulphur, S<sup>-</sup>; oxygen, O<sup>-</sup> and aromatic rings as well as  $\pi$  electrons in their structures.

Amino acids are attractive as corrosion inhibitors because they are relatively easy to produce with high purity at low cost and are non-toxic, biodegradable and completely soluble in aqueous media. Generally, amino acids have two polar groups, namely, one amino group and one carboxyl group. It can coordinate with metals through the nitrogen

atom and oxygen atom of the carboxyl group. It has been shown by a number of investigators that some amino acids can act as corrosion inhibitors, which has generated an increasing interest in these compounds [33-37]. It has the ability to control the corrosion of a wide variety of metals such as pure iron, carbon steel, zinc, mild steel, nickel, copper, lead, aluminum and tin. It behaves as corrosion inhibitor in acid medium, neutral medium and in deaerated carbonate solution. The main objective of the present study is to investigate the protectory effects of the L-Arginine in the corrosion protection of copper in 0.5M HNO<sub>3</sub> using electro chemical methods. Surface analytical techniques were also used to investigate the nature of the surface film. The electronic and molecular structure of protector will be investigated using density functional calculations.

## MATERIALS AND METHODS

### Materials

The specimens of size 1.0cm×4.0cm×0.1cm were press cut from the copper sheet, were machined and abraded with a series of emery papers. This was followed by rinsing in acetone and bidistilled water and finally dried in air. Before any experiment, the substrates were treated as described and freshly used with no further storage. The protector L-Arginine was used as received. A stock solution of 1000ppm of L-Arginine was prepared in bidistilled water and the desired concentration was obtained by appropriate dilution. The study was carried out at room temperature. The structure of L-Arginine is given in Fig 1.

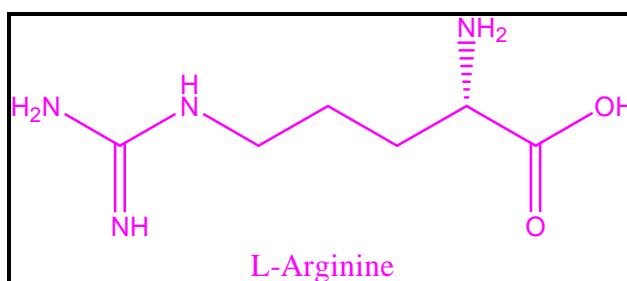


Figure 1. Structure of L-Arginine

### Electrochemical studies

Both the potentiodynamic polarization studies and electrochemical impedance spectroscopic (EIS) studies were carried out using the electrochemical workstation model CHI-660A and CHI-760d and the experimental data were analysed by using the electrochemical software (Version: 12.22.0.0). The measurements were conducted in a conventional three electrode cylindrical glass cell with platinum electrode as auxiliary electrode and saturated calomel electrode as reference electrode.

The working electrode was copper embedded in epoxy resin of polytetrafluoroethylene so that the flat surface of 1cm<sup>2</sup> was the only surface exposed to the electrolyte. The three electrodes set up was immersed in control solution of volume 100ml both in the absence and presence of the inhibitors formulations and allowed to attain a stable open circuit potential (OCP).

Polarization curves were recorded in the potential range of -750 to -150 mV with a resolution of 2mV. The curves were recorded in the dynamic scan mode with a scan rate of 2mV/s in the current range of -20mA to +20mA. The Ohmic drop compensation has been made during the studies. The corrosion potential ( $E_{\text{corr}}$ ), corrosion current ( $I_{\text{corr}}$ ), anodic Tafel slope ( $\beta_a$ ) and cathodic Tafel slope ( $\beta_c$ ) were obtained by extrapolation of anodic and cathodic regions of the Tafel plots. The protection efficiency (PE<sub>p</sub>) values were calculated from the  $I_{\text{corr}}$  values using the equation.

$$(\%) \text{ PE}_p = \frac{I_{\text{corr}} - I'_{\text{corr}}}{I_{\text{corr}}} \times 100$$

Where  $I_{\text{corr}}$  and  $I'_{\text{corr}}$  are the corrosion current densities in case of control and inhibited solutions respectively.

Electrochemical impedance spectra in the form of Nyquist plots were recorded at OCP in the frequency range from 60 KHz to 10MHz with 4 to 10 steps per decade. A sine wave, with 10mV amplitude, was used to perturb the system. The impedance parameters viz., charge transfer resistance ( $R_{\text{ct}}$ ), double layer capacitance ( $C_{\text{dl}}$ ) were obtained from the Nyquist plots. The protection efficiencies (PE<sub>im</sub>) were calculated using the equation,

$$(\%) \text{PE}_{\text{im}} = \frac{R_{\text{ct}} - R'_{\text{ct}}}{R'_{\text{ct}}} \times 100$$

Where  $R_{\text{ct}}$  and  $R'_{\text{ct}}$  are the charge transfer resistance values in the absence and presence of the inhibitor respectively.

#### Water contact angle

In order to evaluate the contact angle experimentally, the sessile droplet method was used. The sessile droplet was rested on a horizontal substrate by a syringe. The substrate was illuminated by a light source, and then a picture was taken by using a high resolution camera (10.1 Mpixel SONY camera). The image was processed by computer by software made for this purpose.

#### Atomic Force Microscopy (AFM)

Atomic force microscopy is a powerful method for the gathering of roughness statistics from a variety of surfaces. This exciting new techniques that allows surface to be imaged at higher resolutions and accuracies than ever before. The protective films are examined for a scanned area. AFM is becoming an accepted technique of roughness investigation [38-41]. AFM provided direct insight into the changes in the surface morphology taking place at several hundred nanometers when topographical changes owing to the initiation of corrosion and formation of protective film onto the metal surface in the with and without addition of inhibitors respectively. All the AFM images were recorded on a Pico SPM2100 AFM instrument operating in contact mode in air. The scan size of all the AFM images are  $15\mu\text{m} \times 15\mu\text{m}$  areas at a scan rate of 0.20(Hz) lines per second.

#### Quantum chemical calculation

The molecular structures of the titled molecule were geometrical optimized using the density functional theory (DFT) method with B3LYP level and 6-31G(d,p) basic set and Gaussian 03W package[42]. Gauss view 3 program has been used to construct optimized molecular geometry HOMO, LUMO energy distributions and HOMO-LUMO energy gap [43, 44].

## RESULTS AND DISCUSSION

#### Weight loss technique

The values of PE% and corrosion rate ( $\text{mmy}^{-1}$ ) obtained from weight loss method at different concentration are summarized in Table 1. It is observed from Figure 1. that PE% increases with increasing the protector concentration in 0.5M  $\text{HNO}_3$  and shows a sharp increase in the protection, which reached its maximum value at concentration of 300ppm and further increase in the protector concentration does not show any appreciable change in the protection efficiency. This indicates that the protective effect of protector is not solely due to their reactivity with the nitric acid. The protectory behaviour of the L-arginine against corrosion of copper can be attributed to the adsorption of protectors on the copper surface, which limits the dissolution of the copper by blocking of its corrosion sites and hence decreasing the corrosion rate from 5.95 to 0.20  $\text{mmy}^{-1}$ .

**Table 1. Weight loss value of various concentrations of L-Arginine in 0.5M  $\text{HNO}_3$  solution**

Conc. of L-Arginine (ppm)	Weight loss ( $\text{mg cm}^{-2}$ )	Corrosion rate ( $\text{mmy}^{-1}$ )	Protection efficiency (%)
Blank	26.3	5.95	-
10	15.0	3.34	44
50	11.5	2.60	56
100	9.0	2.03	65
150	5.0	1.13	81
200	4.0	0.90	85
250	2.3	0.52	90
300	0.9	0.20	97

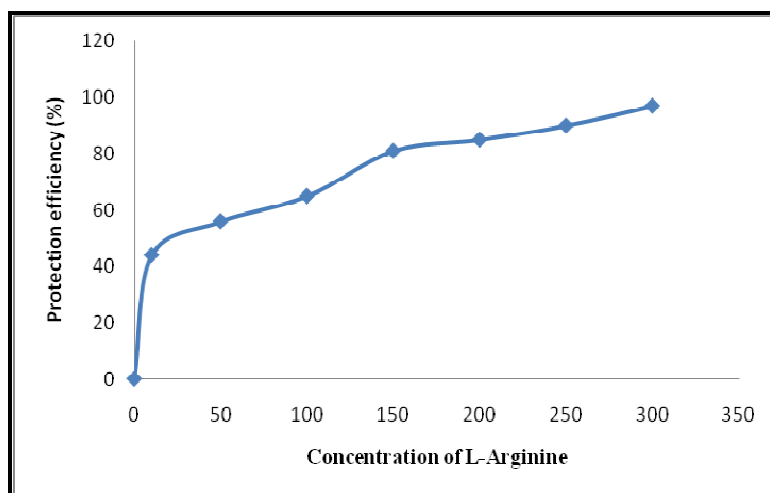


Figure 1. Variation of protection efficiency for copper in 0.5M HNO<sub>3</sub>

### Polarization Technique

The parameters obtained from electrochemical measurements such as corrosion potential ( $E_{\text{corr}}$ ), corrosion current ( $I_{\text{corr}}$ ), anodic and cathodic Tafel slopes ( $\beta_a$  and  $\beta_c$ ) and protection efficiency PE% are given in Table 2.

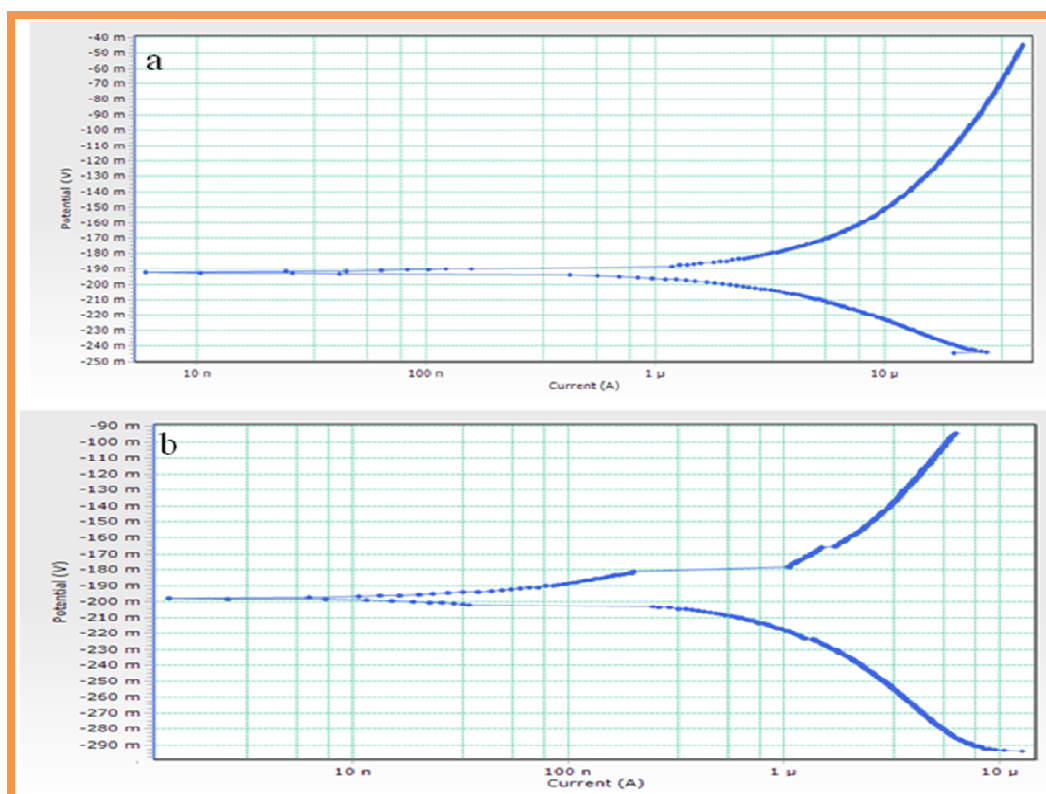


Figure 2. Tafel polarization plots of copper (a) 0.5M HNO<sub>3</sub> solution (blank) (b) 0.5M HNO<sub>3</sub> solutions with 300ppm L-Arginine

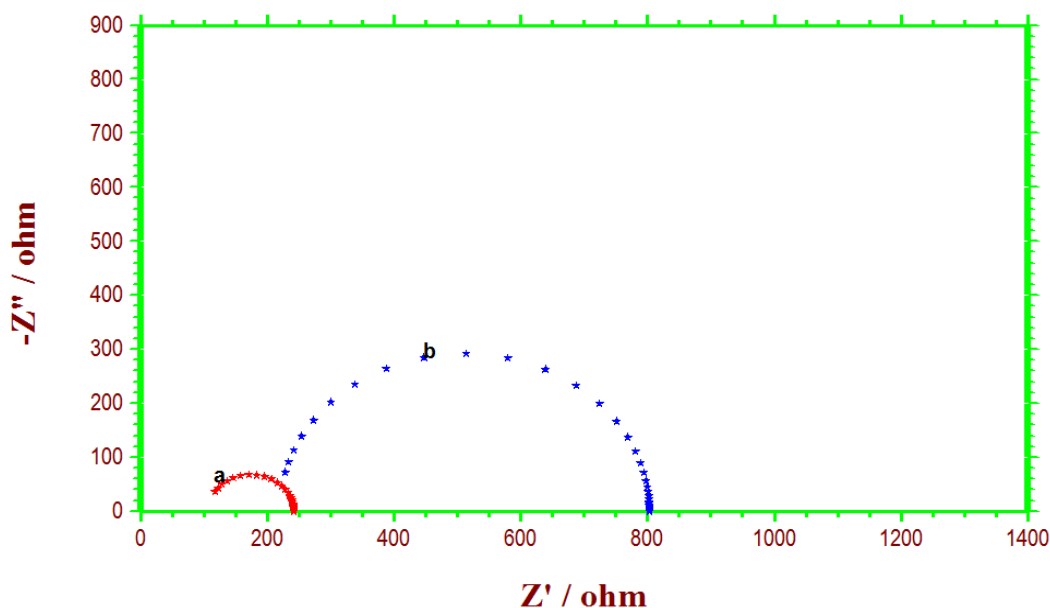
The observed  $E_{\text{corr}}$  values do not change in a regular manner from the blank value. This indicates that the protector works through mixed mode of protection. It is obvious from Figure 2, that Tafel curves are shifted markedly to lower corrosion current density in the presence of protector (300ppm L-Arginine). The  $I_{\text{corr}}$  value decrease from the blank value ( $5.107$  to  $0.183 \times 10^{-6}$ ), this decrease in  $I_{\text{corr}}$  is an indication of increased protection efficiency (96.4). The  $\beta_a$  and  $\beta_c$  slopes values equally shifted in the addition of protector from the blank, which means the L-Arginine molecule acts as a mixed type protector. In other words, both anodic and cathodic reactions of copper electrode are drastically reduced by L-Arginine compound [45].

Table 2. Corrosion parameters for the corrosion of copper in 0.5M HNO<sub>3</sub> in the absence and presence of inhibitor formulation obtained from potentiodynamic polarization technique

Concentration of L-Arginine (ppm)	Tafel parameters				PE <sub>p</sub> (%)
	E <sub>corr</sub> mV vs SCE	I <sub>corr</sub> A/cm <sup>2</sup> ×10 <sup>-6</sup>	β <sub>a</sub> mV/decade	β <sub>c</sub> mV/decade	
Blank	-192.1	5.107	125.5	70.7	-
300	-196.6	0.183	76.9	68.7	96.4

### Electrochemical impedance spectroscopy

The impedance method provides information about the corrosion protection process. Nyquist plots of copper in 0.5M HNO<sub>3</sub> solution in the absence and presence of protector (300ppm L-Arginine) is shown in Figure 3.

Figure 3. Nyquist plots of copper (a) 0.5M HNO<sub>3</sub> solution (blank) (b) 0.5M HNO<sub>3</sub> with 300ppm L-Arginine

The impedance spectra exhibit a small semicircle obtained from blank, and the diameter of semicircle increases in the presence of protector. The Nyquist plots do not present perfect semi-circle, they show a depressed capacitive loop in the high frequency range. These deviation from perfect circular shape, often known as frequency dispersion was attributed to surface roughness and inhomogeneities of the solid surface. Moreover, the impedance response of copper in 0.5M HNO<sub>3</sub> medium alone has changed significantly after addition of the protector. The simplest fitting is represented by Randles electrical equivalent circuits used to fit the experimental results were as previously reported [46-47]. The interfacial double layer capacitance (C<sub>dl</sub>) values have been estimated from the impedance value using Nyquist plots by using the following equation.

$$f(-Z_{\max}'') = \frac{1}{2\pi C_{dl} R_{ct}}$$

This decrease in C<sub>dl</sub> values also indicates the gradual replacement of water molecule by the adsorption of the protector molecule on the metal surface, decreasing magnitude of metal dissolution [48]. The increase in R<sub>ct</sub> from 92.10 Ω to 778.85 Ω value in the presence of 300ppm L-Arginine is due to the formation of protective film on the metal/solution interface. These observations suggest that the resistance toward charge transfer reactions is responsible for corrosion protector process.

Table 3. Electrochemical impedance parameters for copper in 0.5M HNO<sub>3</sub> in the absence and presence of protector

Concentration of L-Arginine (ppm)	Charge Transfer Resistance, R <sub>ct</sub> (Ω)	Double layer capacitance, C <sub>dl</sub> CPE (μF/cm <sup>2</sup> )	IE <sub>imp</sub> (%)
Blank	92.10	40.252	-
300	778.85	0.532	88.17

**Contact angle**

Water contact angle technique analyzed the nature of wettability, whether it's hydrophobic or hydrophilic. Fig 4 shows copper surface immersed in 0.5 M HNO<sub>3</sub>, surface highly porous, more roughness (contact angle 84° ± 2°) and therefore, copper surface is getting hydrophilic nature. Fig 5 shows copper surface immersed in the presence of protector (300ppm L-Arginine); smoother surface appear (contact angle 140° ± 4°) and therefore the surface gets hydrophobic nature. This result confirms the adsorption of a hydrophobic protective film onto the copper surface in the presence of protector.

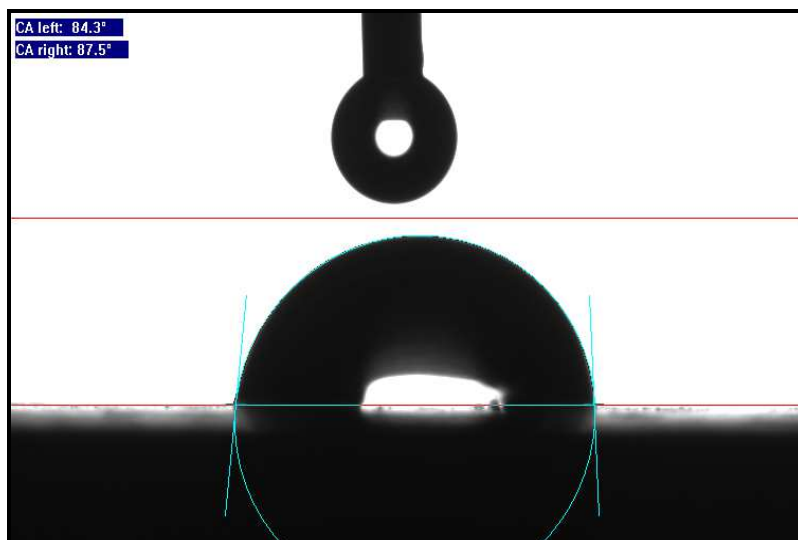


Fig 4. Water contact angle of copper in 0.5M HNO<sub>3</sub> solution

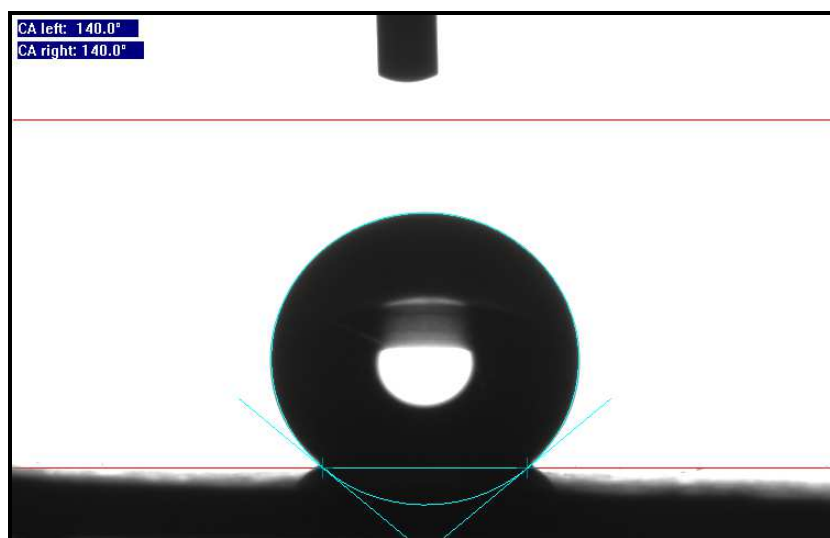


Fig 5. Water contact angle of copper in 0.5M HNO<sub>3</sub> with 300ppm L-Arginine

**Atomic force microscope**

AFM results of copper taken in the absence and presence of protector. In the absence of protector AFM images clearly show a rough surface (maximum surface roughness 3.0µm) due to rapid corrosion of copper in 0.5M HNO<sub>3</sub> solution (Fig 6). In the presence of 300ppm L-Arginine copper is less corroded and a different surface morphology having comparatively smoother surface (maximum surface roughness 0.90µm) is observed in Fig7. A smoother layer with a clearly different morphology is as a result of the formation of a protective layer by the adsorbed protector.

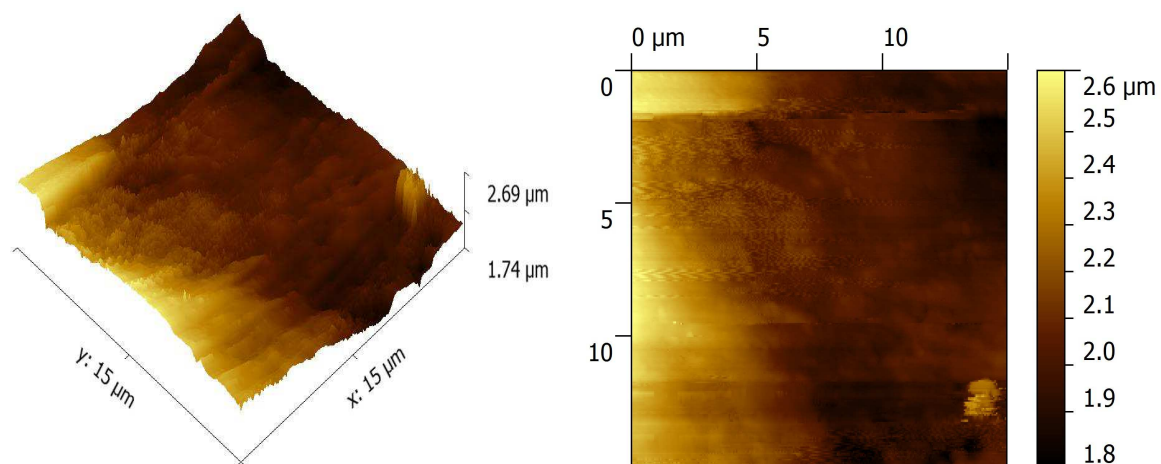
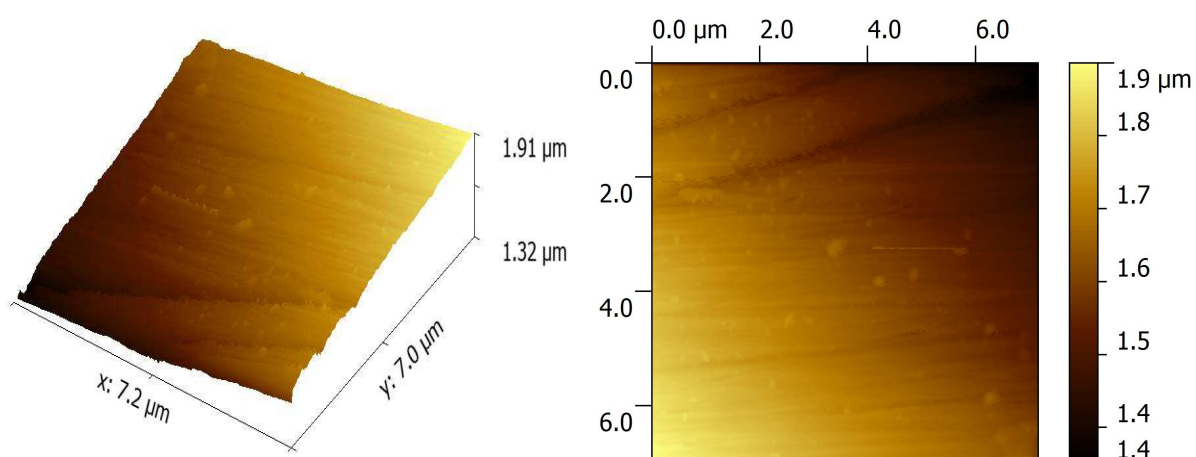
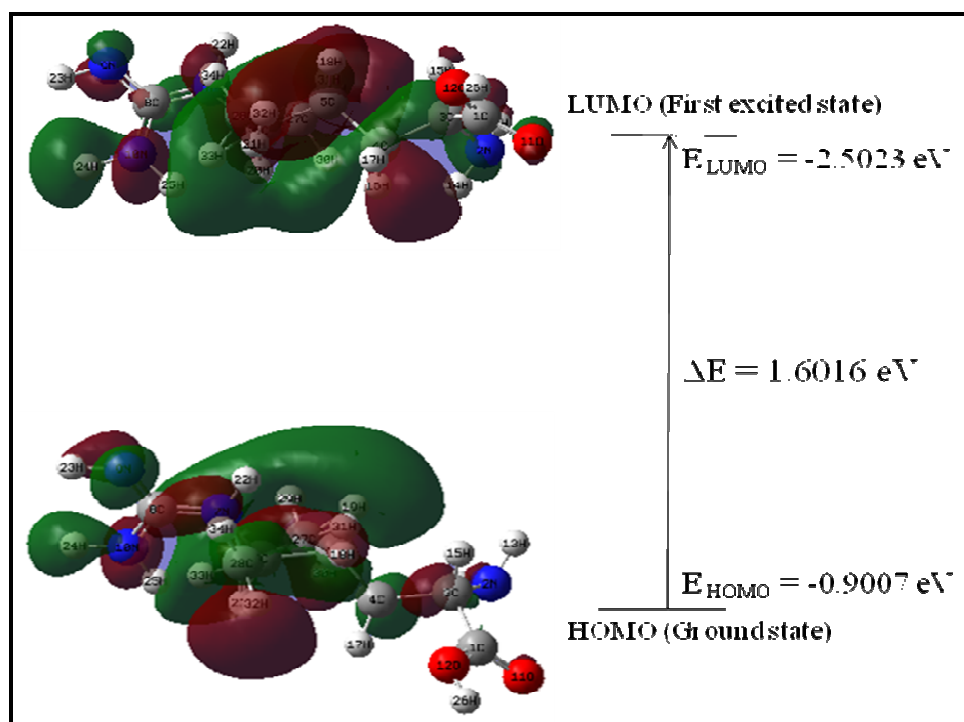
Fig 6. AFM images of copper surface immersed in 0.5 M HNO<sub>3</sub> (blank)Fig 7. AFM images of copper surface immersed in 0.5 M HNO<sub>3</sub> with 300ppm of L-Arginine

Fig 8. Highest occupied and lowest unoccupied molecular orbitals of L-Arginine obtained by B3LYP/6-31G(d,p) method

### Quantum chemical calculations

Quantum chemical calculations were performed to explain the relationship between the molecular structure and the protective action of the protector under study. Fig 8 presents quantum chemical parameters computed for the studied protector, namely energies of the highest occupied molecular orbital (HOMO), lowest unoccupied molecular orbital (LUMO) and energy gap ( $\Delta E = E_{\text{LUMO}} - E_{\text{HOMO}}$ ). The HOMO in L-Arginine is localized mainly around the  $\pi$ -framework, largely on nitrogen atoms and carboxylic group, which enhance electron donation from L-Arginine to the copper surface. Data in Fig 8 reveal that L-Arginine has higher values for both  $E_{\text{LUMO}}$  and  $E_{\text{HOMO}}$  and a tiny ( $\Delta E = 1.6016$  eV) value. A principal decrease in the energy gap leads to easier polarization of the molecule and greater adsorption on the surface [49]. Thus, a tiny  $\Delta E$  in L-Arginine facilitates adsorption, and enhances the protection efficiency.

### CONCLUSION

The following main conclusions are drawn from the present investigation.

1. L-Arginine has good protection efficiency for the corrosion of copper in 0.5M HNO<sub>3</sub> solution.
2. All results obtained from weight loss technique, polarization technique and electrochemical impedance spectroscopy are in reasonably good agreement and shows increased protection efficiency with increasing protector concentration.
3. Polarization technique showed that the investigated protector acts as a mixed type protector on copper in 0.5M HNO<sub>3</sub> solution.
4. Surface analysis using atomic force microscopy (AFM) shows a significant morphological improvement on the copper surface in the presence of protector.
5. Water contact angle showed the hydrophobicity nature of protective film on copper surface.
6. Quantum chemical calculations show that small  $\Delta E$  in L-Arginine facilitates adsorption and enhance the protection efficiency. These observations explain the good adsorption on the copper surface. This theoretical calculation is good agreement with the experimental results.

### REFERENCES

- [1] H.H. Strehblow and B. Titze, *Electrochim. Acta*, **1980**, 25, 839–850.
- [2] M. Finšgar and I. Milošev, *Corros. Sci.* **2010**, 52, 2737–2749.
- [3] F. Mansfeld (Ed.). *Corrosion Mechanisms*, p. 119, Marcel Dekker, New York, **1987**.
- [4] G. TrabANELLI. *Corrosion*, **1991**, 47 (6), 410.
- [5] L. Kiss. *Kinetics of Electrochemical Metal Dissolution*, Elsevir, Amsterdam, **1988**.
- [6] A. Shaban, E. Kálmán, J. Telegdi. *Electrochim. Acta*, **1998**, 43, 159–163.
- [7] A. Jardy, A. Legal Lasalle-Molin, M. Keddám, H. Takenouti. *Electrochim. Acta*, **1993**, 37, 2195.
- [8] A.S. Altaei, *The Iraq Journal for Mechanical and Material Engineering*, **2010**, 10(1), 70-76.
- [9] G. Schmitt, *British Corrosion Journal*, **1984**, 19(4), 165-176.
- [10] P. Rajeev, A.O. Surendranathan, Ch.S.N. Murthy, *Journal of Mater. Environ. Sci.* **2012**, 3(5), 856-869.
- [11] S. John, B. Joseph, K.V. Balakrishnan, K.K. Aravindakshan, A. Joseph. *Materials Chemistry and Physics*, **2010**, 123, 218-224.
- [12] A.M. Simoes, J.Torres, R. Picciochi, J.C.S. Fernandes, *Electrochimica Acta*, **2009**, 54, 3857-3865.
- [13] A. Lesar, I. Milosev, *Chemical Physics Letters*, **2009**, 483, 198-203.
- [14] E.E. Oguzie, S.G. Wang, Y. Li, F.H. Wang, *Journal of Physical Chemistry C*, **2009**, 113 8420-8429.
- [15] F.S. De Sousa, A. Spinelli, *Corrosion Science*. **2009**, 51, 642-649.
- [16] I.L. Lehr, S.B. Saidman, *Electrochimica Acta*. **2006**, 51, 3249-3255.
- [17] E.E. Ebenso, *Journal of Chemical Research*, **2001**, 6, 8-12.
- [18] E.E. Oguzie, G.N. Onuoha, A.I. Onuchukwu, *Materials Chemistry & Physics*. **2005**, 89, 305-311.
- [19] S.A. Umoren, Y. Li, F.H. Wang, *Journal of Solid State Electrochemistry*, **2010**, 14, 2293-2305.
- [20] V. Shinde, S.R. Sainkar, P.P. Patil, *Corrosion Science*. **2005**, 47, 1352-1369.
- [21] P. Pawar, A.B. Gaikwad, P.P. Patil, *Electrochim Acta*. **2007**, 52, 5958-5967.
- [22] R.M. Torresi, S. Solange, J.E. Pereira da Silva, I. Susana, C. Torresi, *Electrochim Acta*. **2005**, 50, 2213-2218.
- [23] S. Souza de, *Surf Coating Technol*, **2007**, 201, 7574-7581.
- [24] R. Vera, R. Schreiber, P. Cury, R. DelRio, *J Appl Electrochem*. **2007**, 37, 519-525.
- [25] G. Xue, Y. Lu, G. Shi, *Appl Surf Sci*. **1994**, 74(1), 37-41.
- [26] T. Tuken, G. Tansug, B. Yazici, M. Erbil, *Surf Coating Technol*. **2007**, 2002, 146-154.
- [27] T. Tuken, B. Yazici, M. Erbil, *Prog Org Coating*, **2005**, 53, 38-45.
- [28] D.P. Schweinsberg, G.A. Hope, A. Trueman, V. Otieno-Alego, *Corrosion Science*, **1996**, 38, 587-599.
- [29] S.A. Umoren, E.E. Ebenso, P.C. Okafor, O. Ogbobe, *Pigment & Resin Technology*. **2006**, 35(6), 346-352.
- [30] S.A. Umoren, I.B. Obot, *Surf. Rev. Lett.* **2008**, 25(3), 277-284.

- [31] J. Shukla, K.S. Pitre, P. Jain, *Ind. Journal of Chem. Soc. A Inorg Phys Theor Anal Chem.* **2003**, 42(11), 2784-2787.
- [32] H. Ashassi-Sorkhabi, N. Ghalebsaz-Jeddi, F. Hashemzadeh, H. Jahani, *Electrochim Acta*, **2006**, 51, 3848-3854.
- [33] D.Q. Zhang, L.X. Gao, G.D. Zhou, *J. Appl. Electrochem*, **2005**, 35, 1081.
- [34] A.B. Silva, S.M.L. Agostinho, O.E. Barcia, G.G.O. Cordeiro, E.D. Elia, *Corros. Sci.*, **2006**, 48, 3668.
- [35] E.E. Oguzie, Y. Li and F.H. Wang, *Electrochim. Acta*, **2007**, 53, 909.
- [36] D.Q. Zhang, Q.R. Cai, L.X. Gao and K.Y. Lee, *Corros. Sci.*, **2008**, 12, 3615.
- [37] J.J. Fu, S.N. Li, L.H. Cao, Y. Wang, L.H. Yan and L.D. Lu, *J. Mater. Sci.*, **2010**, 45, 979.
- [38] Ph. Dumas, B. Butffakhreddine, C. Am, O. Vatel, E. Ands, R. Galindo and F. Salvan, *Europhys. Lett*, **1993**, 22, 717-722.
- [39] J.M. Bennett, J. Jahannir, J.C. Podlesny, T.L. Baiter and D.T. Hobbs, *Appl. Opt.*, **1995**, 43, 213-230.
- [40] A. Duparre, N. Kaiser, H. Truckenbrodi, M. Berger and A. Kohler, *SPIE*, **1993**, 1995, 181-192.
- [41] C. Amra, C. Deumie, D. Torricini, P. Roche, R. Galindo, P. Dumas and F. Salvan Overlapping of roughness spectra measured in microscopic (Optical) and microscopic (AFM) bandwidths, *Int. Symp. On Optical Interference Coatings*, 6-10 June 1994. Grenoble, Proc. SPIE **1994**, 2253, 614-630.
- [42] S. Muthu, T. Rajamani, M. Karabacak and A.M. Asiri, *Spectrochim. Acta A*, **2014**, 122, 1-14.
- [43] M.J. Frisch, A.B. Nielsen, A.J. Holder, *GaussView Users Manual*, Gaussian Inc., Pittsburgh, PA, **2000**.
- [44] D.C. Young, *Computational Chemistry: A Practical Guide for Applying Techniques to Real World Problems (Electronic)*, John Wiley & Sons Inc., New York, **2001**.
- [45] Xianghong Li, Shuduan Deng and Hui Fu, *Corrosion Science*, **2011**, 53, 3241-3247.
- [46] R. Sudhakaran, C. Thangavelu, M. Sekar and T. Kasilingam, *Asian J. Research Chem.* January **2015**, 8(1).
- [47] G. Karthik, M. Sundaravadivelu, P. Rajkumar, *Research on chemical intermediates*, **2013**,  
Doi:10.1007/s11164-013-1291-0.
- [48] A.K. Singh, M.A. Quraishi, *Corrosion science*, **2011**, 53, 1288-1297.
- [49] S.A. Fouda, A.S. Ellithy, *Corros. Sci.*, **2009**, 51, 868-875.